Comparative Analysis of the Source Parameter Imaging and Spectral Depth Techniques of Determining Depth to Magnetic Sources in a Sedimentary Environment, using Aeromagnetic Data.

M.T. Tsepav

Abstract-The results of Spectral Depth Analysis and Source Parameter imaging methods of interpreting Aeromagnetic data in some parts of the Bida basin have been presented and compared.The area falls within latitudes 7.30^0 N and 10. 00^0 N; and longitude 4.00^0E and 7.00^0E. Before using each method, the regional residual separation was done using Oasis montaj to get the residual data for onward processing. The SPI requires the gridding of the residual values and the conversion of this to image map from where depth could be read off easily. The application of SPI delineated the depth to basement rocks within the basin to range from 60.225m to 3.447km while the result of the interpretation of the same data using Spectral Depth Analysis revealed depths to shallow magnetic sources (h_1) ranging from 0.254km to 1.712km covering areas around the southern parts of Kirri and Kotonkarfi magnetic sheets, with an average depth value of about 0.958km. The depth to the deeper magnetic sources, h_2 varied from 1.830km on the northern Kotonkarfi sheet to 4.615 km on the Baro/Gulu magnetic sheets, averaging a depth value of about 3.063km, with the Kainji, Fashe, Mokwa, Egbako, Baro and Patigi/Baro blocks having depths to magnetic sources above 3km. The deeper magnetic sources could be taken as the magnetic basement depth and signify that the basin might be favourable for hydrocarbon accumulation. The shallow source depth can be viewed as magmatic intrusions into the sedimentary basin and could be responsible for the ironstone presence in the area. These methods thus compare favourably well with strong correlation and can be regarded as good automatic source depth determination methods.

Keywords: Aeromagnetic data, Magnetic basement, Spectral Depth, Source Parameter Imaging.

1 INTRODUCTION

Aeromagnetic data analysis is an important tool in determining the magnetic basement depth beneath a sedimentary cover. Most economic minerals, oil, gas, and groundwater lie concealed beneath the earth surface and the presence and magnitude of these resources can be ascertained by geophysical investigations of the subsurface structures in the area. The analysis and the interpretation of geophysical measurements can reveal how the earth's interior varies both vertically and laterally, delineating meaningful information on the geological structures beneath the earth's surface. This information can be used for exploration of a localized region of the upper crust for engineering, hydrogeological and other purposes of interest to man [1]. Of paramount importance in the quantitative interpretation of magnetic data is the depth of the buried anomalous body. This depth can be used in oil and mineral exploration to determine the prospective areas. The Source parameter Imaging (SPI) and Spectral Depth Analysis methods were used to evaluate the depth to basement and compared. These techniques are amongst the modern automatic source depth methods of determining depth to magnetic basement. This work has employed these methods to quantitatively interpret the HRAM data obtained from the most recent (2009) geophysical survey in Nigeria. This work seeks to obtain the magnetic basement depth of the study area, the basement topology and contour orientations and then appraise the hydrocarbon accumulation potential of the

M.T. Tsepav, PhD is currently lecturing in the Department of Physics, Ibrahim Badamasi Babangida University, Lapai, Nigeria.Tel: +2348173967772, E-mail: tsematoo@yahoo.com

basin using these modern approaches. It also looks at how the methods compare between themselves.

2 GEOLOGY OF THE STUDY AREA

The Bida basin (Figure 1) consists of the Bida Sandstone and the Lokoja formation which were produced during the Campanian, the Sakpe, Enagi, Batati, Patti and Agbaja formations which were created during the Maastrichtian. The Bida Formation is divided into the Doko Member and the Jima Member. [2] made a detailed study of the Doko and Jima Members and reported that the Doko Member is about 183m thick and shows localized development of cross-stratification while the Jima Member is about 90m thick and predominantly sandy with extensive cross-stratification. The Doko Member, located 16km south of Bida is the basal unit and consists of 80m of massive and flat bedded arkoses and coarse to medium sandstone with breccia horizons [3]. [4] and [5] also view the member as having fairly to poorly sort and exposed pebbly, sub-arkoses and quartzose sandstones with granular to sub-granular grains which are thought to have been deposited in a braided alluvial fan setting. The sandstones of the Jima Member (Jima Sandstone subfacies), according to [4], are dominantly quartzose, non-arkosic and brownish. Thin intercalations of poorly sort, hard, whitish, argillaceous sandstones are locally present in the lower parts of the Jima subfacies. [4] observed various types of concretions occurring in the sandstone facies from spherical to sub-spherical, sausage-shaped, irregular and compound shapes. Shiny, blackish ferruginous mineral, possibly goethite/haematite, form the cement and some weak to strong concentric growth shells are displayed.

The Sakpe Formation comprises mainly oolitic and pisolitic ironstones with sandy claystones locally, at the base, followed by dominantly oolitic ironstone which exhibits rapid facies changes across the basin at the top [6]. The Enagi Formation as described by [5], on the other hand, consists mainly of siltstones and correlates with the Patti Formation in the Lokoja sub-Basin. Other subsidiary lithologies include sandstone-siltstone with some claystones. Fossil leaf impressions and rootlets have been found within the formation. The formation ranges in thickness between 30m and 60m. Mineral assemblage consists mainly of quartz, feldspars and clay. The Batati formation constitutes the uppermost units in the sedimentary sequence of the Bida Basin. It consists, according to [7], of argillaceous, oolitic and goethitic ironstones with ferruginous claystone and siltstone intercalations and shaly beds which occur in minor proportions some of which have yielded near shore shallow marine to fresh water fauna.

The Lithologic units in Lokoja Formation range from conglomerates, coarse to fine grained sandstones, siltstones and claystones in the Lokoja area [8]. Subangular to subrounded cobbles, pebbles and granule sized quartz grains in the units are frequently distributed in a clay matrix. The outcrops of the Patti Formation occur between Koton-Karfe and Abaji. This formation consists of sandstones, siltstones, claystones and shales interbedded with bioturbated ironstones with the argillaceous units predominating in the central parts of the basin.

The Agbaja Formation forms a persistent cap for the Campanian - Maastrichtian sediments in the Southern Bida Basin as a lateral equivalent of the Batati Formation on the northern side of the basin. It consists of sandstones and claystones interbedded with oolitic, concretionary and massive ironstone beds in this region.

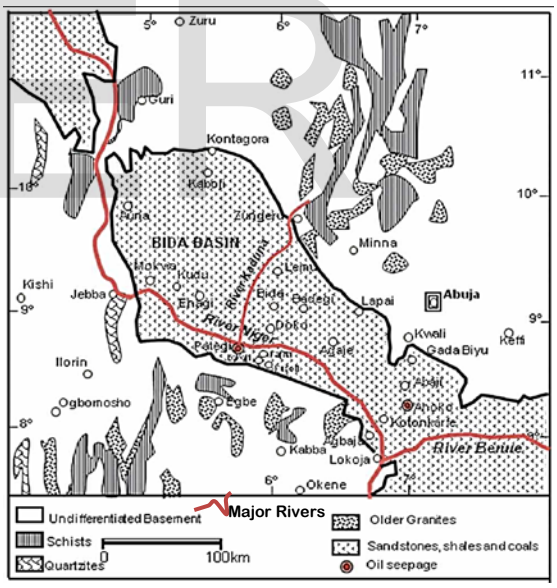

Figure 1: Geology and Location Map of Bida Basin and its Surroundings [5].

3. MATERIALS AND METHODS

3.1: Data Acquisition

The aeromagnetic data used for this work is shown on Figure 2. The IGRF corrected total magnetic field intensity data was acquired from the Nigeria Geological Survey Agency through the Ibrahim Badamasi Babangida

University, Lapai Hydrocarbon Research Project which granted a third party access for the use of the data. Oasis Montaj Software was used to first reduce the data to pole and then Source Parameter Imaging and Spectral Depth Analysis methods were deployed to determine the depth to magnetic rocks.

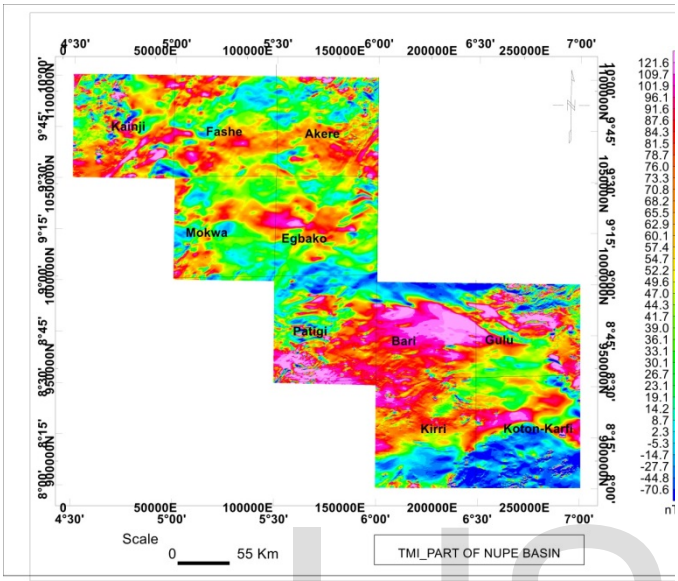

Figure 2: A composite map of the 2009 IGRF Corrected TMI data on sheets covering Parts of the Bida/Nupe Basin

3.2 Reduction to pole

Reduction to the pole (RTP) operation can transform a magnetic anomaly caused by an arbitrary source into the anomaly that the same source would produce if it were located at the magnetic pole and magnetized by induction only. RTP also helps in interpretation of magnetic data by removing the influence of magnetic latitudes and skewness on the anomalies. It is used in low magnetic latitudes to aggregate the peaks of magnetic anomalies to the centre of their sources so that the equivalent of the anomaly appears as if the source was observed at the magnetic north pole. This makes the magnetic anomalies easier to be visualised and interpreted at low latitudes while still retaining the geomagnetic information. RTP is expressed by the equation:

$$L(\theta) = \frac{1}{(sinI_a + icosI.\cos(D-\theta))^2} \qquad (1)$$

where

I is the geomagnetic inclination

I_a is the inclination for amplitude correction which is always greater than one.

D is the geomagnetic declination

The $sinI_a$ term represents the amplitude component while the $icosI.\cos(D-\theta)$ term represents the phase component. In reduction to the pole procedure, the measured total field anomaly is transformed into the vertical component of the field caused by the same source distribution magnetized in the vertical direction. The acquired anomaly is therefore the one that would be measured at the North magnetic pole, where induced magnetization and ambient field both are directed downwards [9].

3.3: The Source Parameter Imaging Method

The Source Parameter Imaging (SPI) method is a technique that uses an extension of the complex analytic signal to estimate magnetic depths. It is profile or grid-based and the solutions show the edge locations, depths, dips and susceptibility contrasts. The method utilizes the relationship between source depth and the local wavenumber (k) of the observed field, which can be calculated for any point within a grid of data through horizontal and vertical gradients [10] with the depth usually displayed as an image. The complex analytic signal $A_1(x,z)$ as defined by [11] is expressed as:

$$A_1(x,z) = \frac{\partial M(x,z)}{\partial x} - j\frac{\partial M(x,z)}{\partial z} \qquad (2)$$

where M(x,z) is the magnitude of the anomalous total magnetic field, j is the imaginary number, and z and x are Cartesian coordinates for the vertical direction and the horizontal direction perpendicular to strike, respectively. [11] showed that the horizontal and vertical derivatives comprising the real and imaginary parts of the 2D analytic signal are related by:

$$\frac{\partial M(x,z)}{\partial x} \Leftrightarrow -j\frac{\partial M(x,z)}{\partial z} \qquad (3)$$

where $\Leftrightarrow$ signifies a Hilberts transform pair. The local wavenumber, k_1, is defined by [10]) as:

$$k_1 = \frac{\partial}{\partial x} tan^{-1}\left(\frac{\partial M}{\partial z} \Big/ \frac{\partial M}{\partial x}\right) \qquad (4)$$

The analytic signal uses the Hilbert transform pair such that the Hilbert transform and the vertical derivative operators are linear. Therefore, the vertical derivative of equation (2) yields:

$$\frac{\partial^2 M(x,z)}{\partial z \partial x} \Leftrightarrow -j\frac{\partial^2 M(x,z)}{\partial z^2} \quad (5)$$

This can be used in defining the analytic signal based on second order derivatives

$$A_2(x,z) = \frac{\partial^2 M(x,z)}{\partial z \partial x} - j\frac{\partial^2 M(x,z)}{\partial z^2} \quad (6)$$

which yields a second order local wave number k_2 given by

$$k_2 = \frac{\partial}{\partial x} tan^{-1}\left(\frac{\partial^2 M}{\partial z^2}/\frac{\partial^2 M}{\partial z \partial x}\right) \quad (7)$$

The first and second – order local wavenumbers are used to determine the most appropriate model and depth estimate independent of any assumption about a model.

[11] derived the expressions for the first and second order local wave numbers as:

$$k_1 = \frac{(n_k+1)h_k}{h_k^2+x^2} \quad (8)$$

and

$$k_2 = \frac{(n_k+2)h_k}{h_k^2+x^2} \quad (9)$$

where n_k is the SPI structural index (subscript k = c, t or h), and n_c=1 and n_h = 2 for the contact, thin sheet and horizontal cylinder models and h_k is the depth to the top of the contact, respectively.

3.4: Spectral Depth Analysis Method

The spectral depths are usually computed from measurement made on the widths and slopes of individual anomalies of the aeromagnetic profiles. The method uses the principle that a magnetic field measured at the surface can be considered to be the integral of magnetic signatures from all depths. The Fourier integral transform of a function that varies continuously along a profile of observation, such as magnetic field intensity, transforms the function from the space to the frequency domain. In its complex form, the two dimensional Fourier transform pair may be written as

$$G(u,v) = \iint_{-\infty}^{\infty} g(x,y)e^{i(u_x - v_y)}dxdy \quad (10)$$

and

$$G(x,y) = \frac{1}{4\pi^2}\iint_{-\infty}^{\infty} g(u,v)e^{i(u_x - v_y)}dudv \quad (11)$$

where u and v are the angular frequencies in x and y directions respectively.

For depth estimations for magnetic field data, this is usually expressed according to [12] as

$$E(u,v)=exp(-4\pi hr) \quad (12)$$

The exp $(-4\pi hr)$ term is the dominant factor in the power spectrum. The average spectrum of the partial waves falling within this frequency range is calculated and the resulting values constitute the radial spectrum of the anomalous field. If we replace h with Z and r with f; then

$$Log\ E = -4\pi Zf \quad (13)$$

where Z is the required anomalous depth; and f the frequency. Therefore the linear graph of logE against f gives slope $m = -4\pi Z$. The mean depth (Z) of the magnetic source is thus given by

$$Z = -\frac{m}{4\pi} \quad (14)$$

The following procedure was employed in the use of this method:

i) *Division of the study area into spectral cells*: The ten residual blocks of the study area were subdivided into 16 spectral blocks (Figure 6) for easy handling of the large data involved.

ii) *Generation of radial energy spectrum*: Oasis Montaj was used to transform the residual magnetic data into the radial energy spectrum for each block.

iii) *Plots of Log of Energy vs the frequency*: The Log-power spectrum of the source has a linear gradient whose magnitude is dependent upon the depth of the source. Graphs of spectral energy against frequencies for the 16 spectral cells were plotted. These series of points which fall on one or more straight line segments represent bodies occurring within a particular depth range. The line segment in the higher frequency range is from the shallow sources and the lower harmonics are indicative of sources from deep seated bodies. The slopes of these graphs in the higher and lower portions of the graphs reveal two depth source models: h_1 and h_2 for shallow and deeper sources respectively. A sample of one of the plots is shown in Figure 7.

iv) *Estimation of the depth to magnetic sources:* The slopes of each of the line segments were first evaluated. The mean depth (h) of burial of the ensemble was then calculated using equation (14).

4. RESULTS AND DISCUSSION

4.1: Result of Reduction to Magnetic Pole (RTP).

Reducing the magnetic data to pole from Oasis Montaj software directly was not achievable as the method introduces drags at the edges of the anomalies, thus complicating the problem of symmetry which results from the dipolar nature of the magnetic data. The problem of drag results because the study area is closer to the equator than the pole. Hence, to achieve TMI reduced to pole, the inverse of the values of IGRF corrected TMI reduced to equator was computed and the result is shown in Figure 3 with the magnetic values ranging from 69.249nT to -121.403nT. From the map, there are some deep pockets of negative and positive anomalies scattered around the region which could be attributed to the undulating topography of the basin which is known to be dominated by sandstones and siltstones which are nonmagnetic, and ironstones which are magnetic in nature.

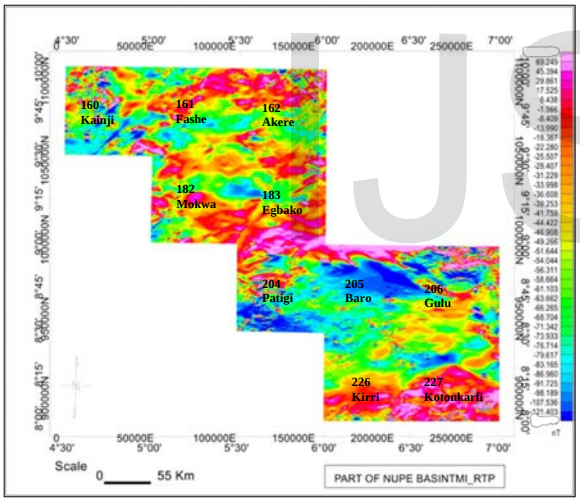

Figure 3: 2009 IGRF Corrected TMI data of Parts of Bida/Nupe Basin Reduced to Pole.

4.2: Source Parameter Imaging (SPI) Result

The result of SPI is displayed as an image and the correct depth estimate for each anomaly can also be determined. Oasis Montaj software was employed to grid the data and compute the SPI image and depth. The results of the depth estimates from application of Source Parameter Imaging method in the study area revealed depth solutions ranging from about 60.225m to 3.447km within the study area. On the SPI depth grid shown in Figure 4, the pink areas indicate the shallowest portions of the basin while the blue portions highlight the deepest pockets. Figure 5 shows a profile plot of SPI depth against lateral distance showing an average estimated depth of about 3.6km. The longest spikes show deep lying bodies and the shortest spikes are indicate shallow seated bodies. It is however, worth noting that since this estimate is only for one profile cutting across only few places in the basin, the actual average depth might be lower.

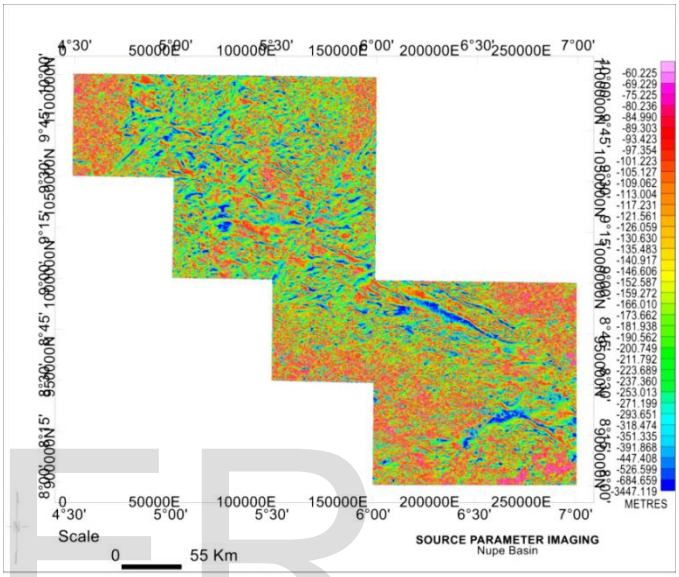

Figure 4: Interpreted Depth to Basement from the 2009 IGRF Corrected AeromagneticData of Bida/Nupe Basin using SPI and indicating the Zones and deepest areas.

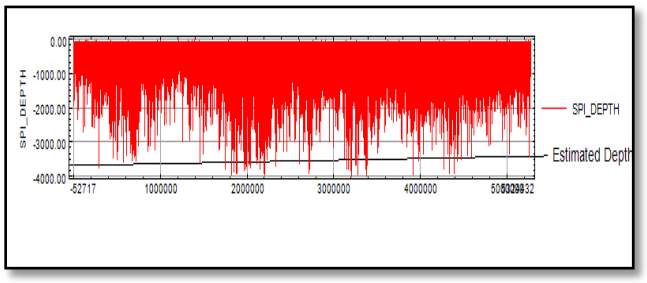

Figure 5: SPI Depth Profile Map

4.3: Result of Application of Spectral Depth Analysis

Spectral Depth Analysis was also applied to the total magnetic field intensity data covering the study area to determine the depth to basement rocks. Regional-residual data separation was performed to distinguish the residual from the regional data.

Figure 6 shows the result of the Spectral Depth Analysis revealing depth to the shallow magnetic sources (h_1) to range from 0.254km on spectral block 9, which is the Kirri magnetic block to 1.719km on the Fashe Block while the depth to the deeper magnetic sources, h_2, varies between a minimum of 1.830 km in section 10 on the Kotonkarfi block and a maximum value of 4.615km on section 15 which lies on the Baro/Gulu interface. The coordinates and the two depth estimates (h_1 and h_2) for each of the sixteen spectral blocks are given on Table 1. Figure 7 is a representation of one of the spectral plots.

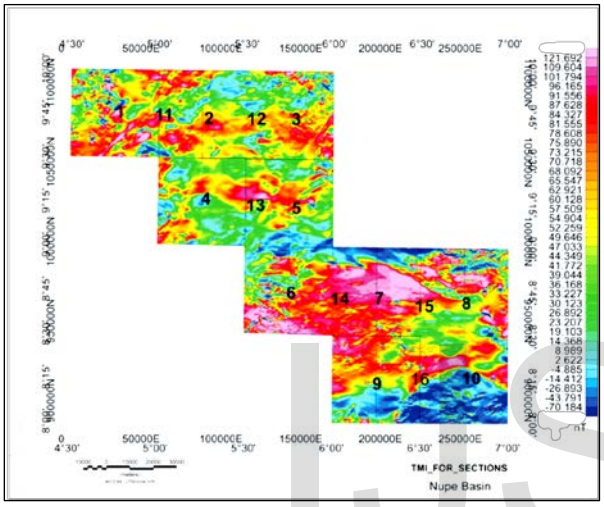

Figure 6 Spectral windows showing the centres of the ensembles

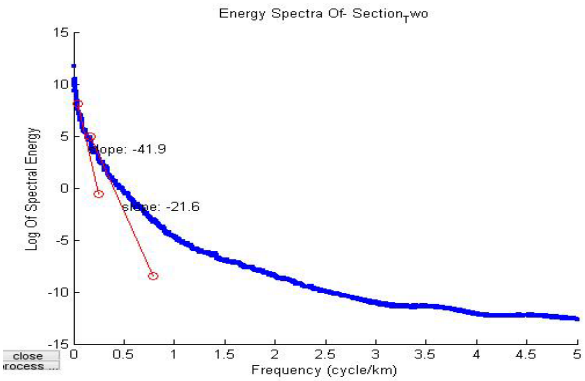

Figure 7: Graphs of Energy spectral vs frequency for Fashe block.

The shallower magnetic sources could be attributed to the presence of near surface magnetic sources which could be magnetic rocks such as laterite, ironstones or ferruginous sandstones or a combination of two or more of these magnetic sources that intruded into the sedimentary section close to the surface. There is also the likelihood of the influence of the adjoining magnetic basement around the study area. The deeper magnetic anomalies on the other hand could be attributed to the presence of intrusions of the magnetic basement into the basin at much deeper depths, lateral discontinuities in the basement and other features differing in magnetic properties such as dykes, faults, fractures, horsts and grabens within the study area.

Figure 8 is the extrapolated map showing depths to deeper sources at a contour interval of 100m. The graphs show succinctly, areas with deep, moderate and shallow depths to magnetic sources, with the deepest magnetic sources identified around the Baro and Gulu spectral blocks and represented by purple to red colour and bounded by latitude 8.60^0N – 9.20^0N and longitude 6.00^0E – 6.60^0E . The areas shown in blue colours around Kainji/Fashe interface block and Kotonkarfi block represent the depths to less deeper magnetic sources. These depths fall within the results obtained by [13], [14], [3], [15], [16] and [17]) as having deeper depths to magnetic sources.

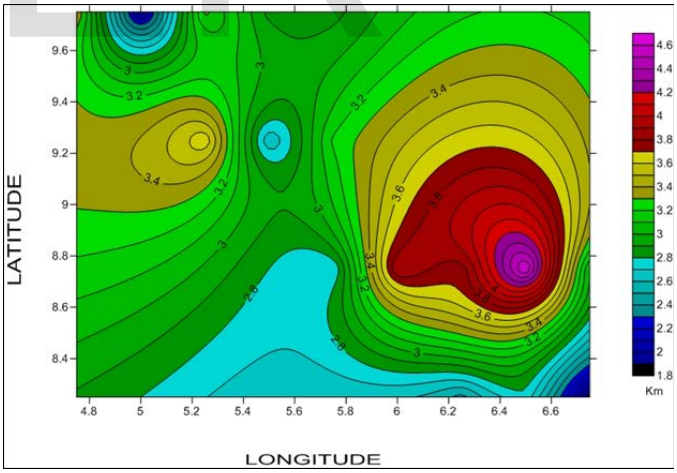

Figure 8: Extrapolated Spectral Depth to Basement Contour map using Surfer 10 software at Contour interval of 1000m.

Table 1: Table of spectral depth for the 16 ensembles of shallow and deeper magnetic sources.

Sections	Long.(Deg. East)	Lat.(Deg. North)	Block Name	Slope (s_1) Shallow Sources	Slope (s_2) Deeper Sources	Depth to Shallow Sources $h_1 = \frac{s_1}{4\pi}$(km)	Depth to Deeper Sources $h_2 = \frac{s_2}{4\pi}(km)$
1	4.75	9.75	Kainji	11.30	42.80	0.899225428	3.4059157822
2	5.25	9.75	Fashe	21.60	41.90	1.718873385	3.3342960578
3	5.75	9.75	Akere	9.25	36.00	0.736091612	2.8647889757
4	5.25	9.25	Mokwa	19.00	46.30	1.511971959	3.6844369326
5	5.75	9.25	Egbako	12.70	40.50	1.010633889	3.2228875976
6	5.75	8.75	Patigi	11.60	34.00	0.92309867	2.7056340326
7	6.25	8.75	Baro	14.00	47.00	1.114084602	3.7401411627
8	6.75	8.75	Gulu	7.71	37.50	0.613542306	2.9841551830
9	6.25	8.25	Kirri	3.19	30.90	0.253852134	2.4589438708
10	6.75	8.25	Kotonkarfi	13.50	23.00	1.074295866	1.8302818456
11	5.00	9.75	Kainji/Fashe interface	11.00	25.40	0.875352187	2.0212677773
12	5.50	9.75	Fashe/Akere interface	11.00	36.00	0.875352187	2.8647889757
13	5.50	9.25	Mokwa/ Egbako interface	15.00	32.80	1.193662073	2.6101410667
14	6.00	8.75	Patigi/Baro interface	13.90	49.00	1.106126854	3.8992961058
15	6.50	8.75	Baro/Gulu interface	12.60	58.00	1.002676141	4.6154933497
16	6.50	8.25	Kiri/Kotonkarfi interface	5.31	34.80	0.422556374	2.7692960098
Minimum depth values (km)						**0.253852**	**1.830282**
Maximum depth values (km)						**1.718873**	**4.615493**

4.4: Comparison between SPI and Spectral depth Techniques

SPI has advantage over Spectral Depth in the sense that SPI is a profile or grid-based method for estimating magnetic source depths and does not require a moving window. In Spectral depth analysis, for small windows of data the limited number of grid nodes often lead to power spectra becoming spikey at the start or end and if this happens, those areas are not considered in determining slopes.

SPI method makes the task of interpreting magnetic data significantly easier as depth can be displayed as an image as shown in Figure 4. The depth estimate can be summarized on one map independent of an assumed model and the computation time is relatively short. However, the interpretation of magnetic data is preferred in frequency domain because of simple relations between

various source models and field [18]. This enables one to use the power spectrum of the surface field to identify average depths of source ensembles as described by [12]. The technique of spectral analysis, therefore, provides rapid depth estimates from regularly- spaced digital field data. No geomagnetic or diurnal corrections are necessary here as these remove only low wave number component and do not affect depth estimate which are controlled by high wave number components of the observed field, [19]. The output of this operation is the radial spectral energy and frequency which can be plotted in straight line graphs and gradients calculation evaluated before depth could be calculated from these gradients.

It could be observed from the application of these automated depth estimating methods that the highest depth estimate of 3.447km obtained in the study area using SPI is lower than the maximum value of 4.615km obtained from spectral depth analysis but can favourably correlate the average value of 3.063km obtained from the spectral analysis. It could further be observed those spectral blocks 2, 4, 5, 7, 14, and 15 which have depth values greater than 3km correspond effectively to the deepest parts observed in the SPI image. Even though a good correlation exists between these results, the SPI result might be more accurate as the observed difference in depth could be attributed to human error which might have been introduced into the spectral analysis when identifying and drawing the lines of best fit on the spectral plots, an action that is carried out manually.

The fact that depth estimates using spectral analysis are referenced to the centre of the ensembles and not along profiles or grids as the case is in SPI, could have also been responsible for the variation in depth estimates using these methods. This is because the assumption that the frequency is evenly distributed in any given spectral block is to some extent overgeneralization. Another factor which might have given rise to the depth discrepancy is the established principle by Spector and Grant (1970) that errors in depth estimation increase as the depth of the causative magnetic bodies also increases and vice versa. The deep seated magnetic bodies might have therefore, been determined with some measure of error due to this principle.

5 CONCLUSION

The research has effectively revealed the depths to magnetic basement with the aid of Source Parameter Imaging and Spectral Depth Analysis methods using aeromagnetic data of some areas around the Bida Basin of Nigeria. The SPI method gave a range of depth values from about 60.225m to 3.447km within the study area. The application of Spectral Depth Analysis, on the other hand, revealed depths to the shallow magnetic sources (h_1) to range from 0.254km on spectral block 9, which is the Kirri magnetic block to 1.719km on the Fashe Block while the depth to the deeper magnetic sources, h_2, varies between a minimum of 1.830 km in section 10 on the Kotonkarfi block and a maximum value of 4.615km on section 15 which lies on the Baro/Gulu interface, with most of the blocks having depths obove 3km. The shallower magnetic sources could be attributed to the presence of near surface magnetic sources which could be magnetic rocks such as laterite, ironstones or ferruginous sandstones or a combination of two or more of these magnetic sources that intruded into the sedimentary section close to the surface. There is also the likelihood of the influence of the adjoining magnetic basement around the study area. The deeper magnetic anomalies on the other hand could be attributed to the presence of intrusions of the magnetic basement into the basin at much deeper depths, lateral discontinuities in the basement and other features differing in magnetic susceptibilities such as dykes, faults, fractures, horsts and grabens within the study area. Based on these results, the deepest areas with sedimentary thickness values obove 3km such as Fashe, Akere, Mokwa, Egbako, Baro, Gulu, Kainji, Patigi and Kotonkarfi should be further investigated for hydrocarbon potential.

REFERENCES

[1] Keary P, Brooks M (1984). An Introduction to Exploration Geophysics. Blackwell Scientific Publications.
[2] Adeleye, D. R. (1974). Sedimentology of the fluvial Bida Sandstones (Cretaceous) Nigeria. *Sedimentary Geology*, 12, 1-24. http://dx.doi.org/ 10.1016/0037-0738(74)90013-X.
[3] Olaniyan, O., Abbah, U., Nwonye, N., Alichi, A. and Udensi, E.E. (2012). Interpretation of Total Magnetic Intensity Field over Bida Basin. Nigerian Geological Survey Agency. *Occasional Paper* No. 15. 98p.
[4] Adeleye, D. R. (1989). The Geology of the middle Niger basin. In: Kogbe, C.A. (Ed.), Geology of Nigeria, second ed. Elizabethan Publishing Co., Lagos, 335–338.

[5] Obaje N. G. (2009). Geology and Mineral Resources of Nigeria, Lecture Notes in Earth Sciences. Springer Dordrecht Heidelberg, London New York. 221p.

[6] Adeleye, D. R. (1973). Origin of ironstones, an example from the middle Niger Basin, Nigeria. *Journal of Sedimentary Petrology* 43, 709–727.

[7] Obaje, N. G., Balogu,D. O., Idris-Nda, A., Goro, I. A., Ibrahim, S. I., Musa, M. K. Dantata, S. H., Yusuf I., Mamud-Dadi, N. and Kolo I. A (2013). Preliminary Integrated Hydrocarbon Prospectivity Evaluation of the Bida Basin in North Central Nigeria. *Petroleum Technology Development Journal*, 3 (2), 36-65.

[8] Akande, S.O., Ojo, O.J., Erdtmann, B.D. and Hetenyi, M. (2005). Paleoenvironments, organic petrology and Rock-Eval studies on source rock facies of the Lower Maastrichtian Patti Formation, southern Bida Basin, Nigeria. *Journal of African Earth Sciences,* 41, 394–406.

[9] Blakely RJ (1995) Potential Theory in Gravity and magnetic application. Cambridge: University Press70: 285-3003.

[10] Thurston, J. B., and Smith, R. S. (1997). Automatic conversion of magnetic data to depth, dip, and susceptibility contrast using the SPI™ method. *Geophysics* (62) 807- 813.

[11] Nabighian, M. N. (1972). The analytic signal of two dimensional bodies with polygonal cross section: Its properties and use for automated anomaly interpretation. Geophysics, 37, 507–517.

[12] Spector, A., and Grant, F.S. (1970), Statistical Models for interpreting aeromagnetic data. *Geophysics* Vol. (35), 293-302.

[13] Ojo, S. B. (1990). Origin of a major magnetic anomaly in the Middle Niger Basin, Nigeria. *Tectonophysics, 85*, 153-162. dx.doi.org/10.1016/0040-1951(90)90410-A

[14] Udensi, E. E. and Osazuwa, I. B. (2004). Spectra determination of depths to magnetic rocks under the Nupe basin, Nigeria. Nigeria Association of Petroleum Explorationists (NAPE) Bulletin 17, 22–27.

[15] Ofor, N. P., Adam, K. D. and Udensi, E. E. (2014). Spectral Analysis of the Residual Magnetic Anomalies Over Pategi and Egbako Area of the Middle Niger Basin. *Nigeria. Journal of Natural Sciences Research*, 4(9), 44-50.

[16] Ojo, S. B. and Ajakaiye, D. E. (1989). Preliminary interpretation of gravity measurements in the middle Niger Basin area, Nigeria. In: Kogbe, C.A. (Ed.), Geology of Nigeria, second ed. Elizabethan Publishing Co., Lagos, 347–358p.

[17] Obi, D. A., Ilozobhie A. J. and Abua J. U. (2015). Interpretation of aeromagnetic data over the Bida Basin, North Central, Nigeria. *Advances in Applied Science Research*. 6(3), 50-63.

[18] Kearey, P, Brooks, M. and Hill, I. (2004), An Introduction to Geophysical Exploration. Third Edition, Blackwell Pub. 281p.

[19] Naidu P.S, Mathew M.P. (1998). Analysis of geophysical potential fields, A digital signal processing approach. Elsevier Science publishers, Amsterdam.